San Miguel, V., Limer, A. J., Haddleton, D. M., Catalina, F. & Peinado, C. (2008): Biodegradable and thermoresponsive micelles of triblock copolymers based on 2-(N,N-dimethylamino)ethyl methacrylate and ε-caprolactone for controlled drug delivery. *European Polymer Journal*, 44 (11), pp. 3853-3863.

DOI: 10.1016/j.conbuildmat.2015.04.060

Biodegradable and thermoresponsive micelles of triblock copolymers based on 2-(*N*,*N*-dimethylamino)ethyl methacrylate and ε-caprolactone for controlled drug delivery

Verónica San Miguel [a], A.J. Limer [b], D.M. Haddleton [b], Fernando Catalina [a], Carmen Peinado [a,*]

[a] *Instituto de Ciencia y Tecnología de Polímeros, C.S.I.C., C/Juan de la Cierva 3, 28006 Madrid, Spain*
[b] *Department of Chemistry, University of Warwick, Coventry CV4 7L, UK*

Abstract

Amphiphilic triblock copolymers, poly(2-(*N*,*N*-dimethylamino)ethyl methacrylate)$_x$-*block*-poly(caprolactone)-*block*-poly(2-(*N*,*N*-dimethylamino)ethyl methacrylate)$_x$, PDMAEMA$_{Co}$, were synthesized. Polymerization and structural features of the polymers were analyzed by different physicochemical techniques (GPC, ^{1}H NMR and FTIR). Formation of hydrophobic domains as cores of the micelles was studied by ^{1}H NMR and further confirmed by fluores-cence. Dynamic light scattering measurements showed a monodispersed size distribution only for the copolymer with the lowest degree of polymerization, while increasing the length of PDMAEMA blocks leads to a bimodal size distribution. The micelles showed reversible dis-persion/aggregation in response to temperature cycles through an outer polymer shell lower critical solution temperature (LCST) for PDMAEMA at temperatures between 54 and 87 °C. The triblock copolymer micelles were loaded with the sparingly water-soluble anticancer drug, chlorambucil, by a dialysis procedure. The drug release profile monitored by fluores-cence showed that the release of chlorambucil from PDMAEMA nanoparticles is controlled by a combined degradation–diffusion mechanism.

Keywords: Block copolymer - Micelles - Temperature sensitivity - Controllable drug release - Chemotherapy

1. Introduction

Amphiphilic block copolymers contain hydrophobic blocks covalently linked to hydrophilic blocks [1]. The repulsion between the dissimilar groups leads to microphase segregation into different domains. The chemical connectivity between blocks and minimization of interfacial energy defines the limits of these domains which are on the nanoscopic scale. In solution the interaction between polymer and solvent adds an extra dimension to the phase separation behaviour, especially when the solvent is selective: a poor solvent for at least one of the blocks and a good solvent for the others. Analogous to smaller surfactant molecules, amphiphilic block copolymers self-assemble in an aqueous milieu in order to minimize contact between hydrophobic segments and water. Self-assembly begins when the copolymer concentration reaches a threshold value known as the critical micelle concentration (cmc). The morphology of the resulting microstructure depends heavily on molecular architecture [2] and micelles are the most common morphology.

Recently, polymer micelles have received increasing attention, not only due to their unique morphological behaviour, but also for their potential in drug delivery [3–6]. The goal of chemotherapy is to deliver an anticancer agent, typically a small molecule, at a high dose to a tumor to kill rapidly proliferating tumor cells. Unfortunately, the maximum dose of many chemotherapeutic agents is limited by their high levels of systemic toxicity in normal tissues, so that the administered dose is frequently suboptimal for effective therapy. Consequently, a number of approaches

* Corresponding author.
E-mail addresses: vsanmiguel@ictp.csic.es (V. San Miguel), D.M.Haddleton@warwick.ac.uk (D.M. Haddleton), fcatalina@ictp.csic.es (F. Catalina), cpeinado@ictp.csic.es (C. Peinado).

have been investigated to decrease the systemic toxicity and increase the therapeutic index of anticancer drug by directly targeting the tumor with macromolecular drug carriers. In particular biodegradable amphiphilic block copolymers for polymeric delivery devices serve as unique materials to overcome some of these problems. Owing to their small size and excellent biocompatibility, nanosized polymers bearing therapeutic agents can circulate in the bloodstream for prolonged periods of time, allowing them to reach the target site and improving the therapeutic efficiency of drugs. In addition, micelles in aqueous solutions are formed by a hydrophobic core, which may serve as container for poorly water-soluble drugs. The corona micelle determines interactions with the external environment which depends on the chemical and physical nature of the hydrophilic block.

Another key issue in anticancer drug delivery is the targeting strategy. It has been demonstrated that polymeric micelles based drug nanocarriers can preferentially and effectively accumulate in solid tumors. This phenomenon is explained by the microvascular hyperpermeability to circulating macromolecules and their impaired lymphatic drainage in solid tumors, and is termed the "Enhanced Permeability and Retention (EPR) effect". Active tumor targeting may be achieved by stimuli-responsive micelles that release their drug load in response to environmental or physical stimuli, such as the lower of pH in the tumor tissue, heat sound or light. For example, thermosensitive drug carrier undergoes a structural transition as a response of temperature increase, resulting in the deposition of the drug and easier drug absorption by cells. Most of the thermosensitive micelles are known to aggregate below physiological temperature (37 °C) and therefore, they deposit as soon as they are injected in the body. A good choice is to use micelles with a LCST (lower critical solution temperature) above the temperature of clinical hyperthermia (above 40 °C). This type of the thermoresponsive micelles can release a drug on demand in response to a local tumor heating to the LCST by, for example, continuous wave ultrasound.

Hydrophilic blocks commonly used in drug delivery include polyethers such as poly(propylene oxide) and PEG [7,8]. Other hydrophilic polymers may be used such as poly(2-(*N,N*-dimethylamino)ethyl methacrylate) (PDMAEMA) due to its biocompatibility, pH sensitivity [9–11] and thermoresponsiveness [12–14]. Recently, well-defined dendritic star-block-poly(ι-lactide)b-poly(2-(*N*, *N*-dimethylamino)ethyl methacrylate) copolymers have been prepared [15]. These systems have been proved useful as drug release vehicles and the release rate of an anticancer drug was effectively controlled by altering the pH of the medium. In spite of the potential cytotoxicity, water-soluble polycations have been described for various technical and biomedical applications [16].

Nanocarriers used for drug delivery need to be biodegradable, biocompatible, non-immunogenic and physically stable in blood stream. Poly(ε-caprolactone), PCL, is an aliphatic polyester of interest for biomedical applications owing to its good compatibility, low immunogenicity and FDA approval. For drug release applications, the advantages of PCL include its favourable permeability to drugs and less acidic degradation products as compared to polylactide and polyglycolide [17]. PCL is a biodegradable polymer and can undergo hydrolytic degradation. However, PCL has suffered from the lack of controlled degradation due to its crystallinity and hydrophobicity. Introduction of hydrophilic units have used to improve biodegradability and hydrophilicity.

A considerable effort has been carried out in the last decade to relate the structure and micellar characteristics to the drug loading and release behaviour from block copolymers. In this study, we explore the potential of the novel micelles as a drug delivery vehicle for lipophilic drugs and analyze the effects that the chemical structures of the shell-forming hydrophilic block have on drug incorporation. For this purpose, we synthesized three different triblock copolymers poly(dimethylaminoethyl methacrylate)$_x$-block-poly(caprolactone)-block-poly(dimethylaminoethyl methacrylate)$_x$ by ATRP (atom transfer radical polymerization) using a difunctional macroinitiator based on poly(caprolactone). And the micellization behaviour has been studied by ^{1}H NMR, fluorescence, TEM and dynamic light scattering (DLS).

To evaluate the controlled drug delivery properties of copolymer aggregates, chlorambucil, an anticancer drug was used as a model because of its very low solubility in water. Chlorambucil is a derivative of nitrogen mustard and acts as a cell cycle phase non-specific bifunctional alkylating agent. Alkylation takes place through the formation of a highly reactive ammonium radical. This radical likely forms a cross-linkage between two strands of DNA, interfering with DNA, RNA and protein synthesis. Their primary uses are chronic lymphocytic leukemia, Hodgkin's lymphoma, Non-Hodgkin's lymphoma and also is used in ovarian cancer. Enhancement of therapeutic efficiency of highly hydrophobic drugs may be achieved by improving their solubility. Moreover, chlorambucil exhibits fluorescence emission which allows monitoring drug release by fluorescence measurements.

2. Experimental section

2.1. Materials

Poly(caprolactone) diol (Aldrich, $M_n \sim 2000$ g/mol), 2-bromoisobutyryl bromide (Aldrich, 98%), triethylamine (TEA, Fischer, 99%, stored over potassium hydroxide pellets), iodomethane (Aldrich, 99%) were used as received without further purification. 2-(dimethylamino)ethyl methacrylate (DMAEMA, Aldrich, 99%) was purified by passage through a short column of activated basic alumina before use to remove inhibitors and acidic impurities. Copper bromide (Cu(I)Br) (Aldrich, 99%) was purified according to the method of Keller and Wycoff [18]. *N*-(Propyl)-2-pyridylmethanimine was prepared as described earlier [19]. Toluene (BDH, 98%) was degassed by bubbling with nitrogen for 30 min and water used in all experiments was MilliQ-grade. Bovine serum albumin (BSA, >95%, $M_n \sim 66$ kDa, fraction V) was purchased from Sigma.

2.2. Synthesis of amphiphilic copolymers

ABA triblock copolymers with different lengths of DMAEMA were synthesized via a two-step reaction (Fig. 1).

Firstly, a dihydroxy PCL was end-functionalized using 2-bromoisobutyryl bromide. The resulting polymer was used as macroinitiator in the polymerization of DMAEMA leading to triblock copolymers with a central core of PCL and PDMAEMA as terminal blocks of different lengths. A similar experimental procedure was recently reported [20].

2.2.1. Synthesis of macroinitiator

2-Bromoisobutyryl bromide (9.3 mL, 75 mmol) and triethylamine (10.5 mL, 75 mmol) were added to an anhydrous THF solution (300 mL) of α, ω-hydroxy terminated poly-ε-caprolactone (M_n = 2000 g/mol) under a nitrogen atmosphere. The reaction was carried out at ambient temperature overnight. The precipitated salts were removed via filtration and volatiles removed under reduced pressure. The obtained viscous oil product was dissolved in dichloromethane and washed with saturated $NaHCO_3$ solution. The organic phase was dried over anhydrous magnesium sulphate and removed. The solid and white product was eluted through a basic alumina column with dichloromethane (yield = 70%).

2.2.2. Synthesis of triblock copolymers

Three block copolymers were synthesized by changing the feed composition. The ratio between the concentrations of initiator, catalyst and ligand were maintained constant in all the polymerizations ([I]:[C]:[L] = 1:2:4.2). The ratios of monomer concentration to initiator were 70:1 for $PDMAEMA_{co}(30)$; 60:1 for $PDMAEMA_{co}(25)$ and 50:1 for $PDMAEMA_{co}(20)$.

A typical polymerization procedure is detailed below. PCL based macroinitiator (2 g, 0.88 mmol) was placed in a Schlenk tube and dissolved in deoxygenated toluene (24 mL). 2-(*N*,*N*-dimethylamino)ethyl methacrylate (10.4 mL, 61.6 mmol) was added to the solution. Then, the tube was sealed with a rubber septum and the mixture degassed via three freeze-pump-thaw cycles. Cu(I)Br (0.25 g, 1.76 mmol) was added to the frozen mixture and it was deoxygenated by three vacuum-N_2 cycles. The reaction mixture, under an atmosphere of nitrogen, was placed in an oil bath at 80 °C. Once the solution reached the desired reaction temperature of 80 °C, *N*-propyl-2-pyridinylmethyleneamine (0.59 mL, 3.69 mmol) (t = 0) was added. The reaction mixture immediately turned dark brown in colour in addition of the ligand. Samples were removed periodically throughout the reaction in order to follow the polymerization by ^{1}H NMR in $CDCl_3$ and GPC. Polymerization was finished after 4 h by exposing the reaction solution to air, leading to aerial oxidation of the catalyst. Catalyst residues were removed by filtering through an activated basic alumina column. The volatiles were removed by rotary evaporation and under high vacuum at ambient temperature.

2.2.2.1. ^{1}H NMR ($CDCl_3$, 400 MHz). δ (ppm): 0.90 (3H, m, CH_3–$C_{PDMAEMA}$), 1.40 [28H, m, 14OC–$(CH_2)_3$–CH_2–CH_2O_{PCL}], 1.65 [56H, m, 14OC–CH_2–$(CH_2)_2$-$(CH_2)_2$–O_{PCL}], 1.85 (12H, s, $4CH_{3\,PCL}$), 1.95 (2H, m, Br–CH_2–$C_{-PDMAEMA}$), 2.30 [28H, m, 14OC–CH_2–$(CH_2)_4$–O–$_{PCL}$], 2.30 [6H, m, –N–$(CH_3)_{2\,PDMAEMA}$], 2.55 (2H, m, –CH_2–$N_{PDMAEMA}$), 3.65 [4H, m, 2O–CH_2–CH_2–

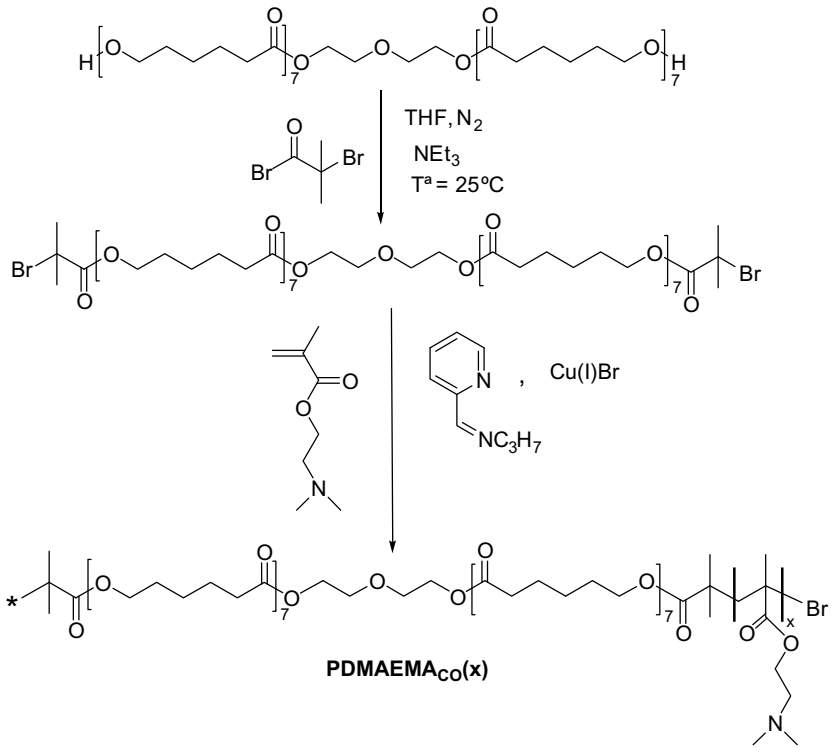

Fig. 1. Scheme of synthesis of the triblock copolymers based on 2-(*N*,*N*-dimethylamino)ethyl methacrylate and ε-caprolactone.

OCO_{PCL}], 4.05 [24H, m, 12OC–$(CH_2)_4$–CH_2O_{PCL}], 4.05 (2H, m, –COO–CH_2–$_{PDMAEMA}$), 4.20 [4H, t, 2O–CH_2–CH_2–OCO_{PCL}], 4.35 [4H, m, 2OC–$(CH_2)_4$–CH_2,OCO_{PCL}].

2.2.2.2. IR (KBr). ν (cm^{-1}): 2950 (st, C–H), 2824 (st, O–CH_2), 2772 [N–$(CH_2)_2$–O_{DMAEMA}], 1730 (O–$C{=}O_{DMAEMA}$), 1460, 1274 (PDMAEMA), 1154 (H_2C–O–CH_2), 750 [γ, C–$(CH_2)_n$–C_{PCL}].

2.2.3. General procedure for quaternization of PDMAEMA triblock copolymers with MeI

Polymer (1 g) was dissolved in dichloromethane (50 mL) at 25 °C under an atmosphere of nitrogen. Methyl iodide (1.71 g, 12 mmol) was added and the mixture was stirred vigorously at 25 °C for 24 h. Precipitation of the polymer starts to occur after ~20–30 min. The reaction mixture was filtered and the quaternized $PDMAEMA_{co}Q(x)$ polymer was dried under vacuum.

2.2.4. General procedure for quaternization of PDMAEMA triblock copolymers with HCl

Polymer (2.9 g) was dissolved in 100 mL of water and 40 mL of 0.5 M HCl (aq) with stirring. The solution was frozen in liquid nitrogen and lyophilized to give the corresponding chlorohydrated $PDMAEMA_{co}Cl(x)$ copolymers.

2.3. Optical transmittance measurements

Optical transmittance of PDMAEMA block copolymer (1.5 g/L) in phosphate buffer solution (PBS, 0.01 M, pH 7.4 and pH 6.4) at various temperatures was measured at 550 nm with a Lambda 32 UV–vis spectrometer (Perkin-Elmer). The sample cell was thermostated in a refrigerated circulator bath at different temperature from 10 to 90 °C prior to measurements. The LCST of the polymer solution was defined as the temperature producing a half decrease of the total decrease in optical transmittance.

2.4. Fluorescence measurements

The cmc's were determined by a fluorescence probe technique using 4-(*N,N*-diethyl) amino-7-nitrobenz-2-oxa-1,3-diazole (NBD-NEt_2) as a fluorescent probe, synthesized as previously described [21]. Fluorescence emission spectra were recorded on a Perkin-Elmer LS-50B spectrofluorimeter. All measurements were performed at 20 ± 1 °C. To improve the accuracy in the determination of maximum wavelengths first derivative spectra were obtained in all of the wide emission bands. Sample solutions were prepared by dissolving a known amount of polymer in water, from 2×10^{-3} to 20 g/L. As the employed fluorescent probe exhibits low solubility in water, *stock* solutions were prepared in ethanol. The stock solution (2.2×10^{-3} M) was added into the examined polymer water solutions of a given concentration in amounts less than 1.5 vol.%, and the solutions were allowed to stand 1 day for equilibration. The effective concentration of probe was maintained at 4×10^{-6} M in all the aqueous solutions. Fluorescence emission spectra of the probe were recorded in the range 490–700 nm using a fixed excitation wavelength of 477 nm. Under such experimental conditions, only one single fluorescence emission peak was observed. All the spectra were corrected using the response curve of the photomultiplier.

2.5. Dynamic light scattering (DLS)

Solutions for light scattering measurements were prepared by dissolving the triblock copolymer in previously filtered, distilled deionized water. DLS measurements were performed using a Malvern Zetasizer 3000 spectrometer equipped with a 5 mW helium neon laser operating at 633 nm. All measurements were carried out with 5 g/L copolymer solution at a scattering angle of 90° and at ambient temperature. The aggregates sizes were determined with the data fitted with CONTIN algorithm as supplied by Malvern Instruments.

2.6. Transmission electron microscopy (TEM) measurements

TEM images were obtained using an electron microscope Philips Tecnai 20T operating at 200 kV. To prepare the TEM samples, 5 microL of an aqueous solution of block copolymer micelles was dropped onto a carbon-coated copper grid and the water droplet was allowed to evaporate slowly in air.

2.7. Drug loading

The triblock copolymers (60 mg, 1% w/v) were dissolved in 6 mL of a phosphate buffer solution (PBS, 0.01 M, pH 7.4). Solution was stirred in the dark overnight. Chlorambucil was dissolved in ethanol. Specific volumes of the drug and copolymer stock solutions were mixed to achieve a final copolymer concentration higher than cmc and drug to polymer ratio of 1:5 (w/w). Drug concentration was varied from 1 to 160 μM. The copolymer-drug solutions were stirred for 4 h, and then placed in a dialysis cell (molecular weight cut-off: 1000 g/mol, *Spectrapore*). Excess of drug was removed by dialysis against PBS solution (0.01 M, pH 7.4) during 24 h. To determine the entrapment efficiency, the drug loaded micelles solution was lyophilized and then, dissolved in ethanol. The loaded aggregates were disrupted by the addition of ethanol (micellar solution: ethanol ratio, 1:2500, v/v).

The loading efficiency of chlorambucil incorporated into the triblock copolymer micellar aggregates was determined by fluorescence. The fluorescence assay included measurement of the emission intensity at 348 and 338 nm with an excitation wavelength of 305 nm. By plotting emission intensity at 348 nm as a function of concentration a standard curve for chlorambucil in PBS solution was prepared over the concentration range of 5×10^{-2}–6×10^{-3} g/L. A second standard curve was obtained over the concentration range 5×10^{-3}–10^{-6} g/L, using the emission intensity at 338 nm. Both curves showed correlation coefficients higher than 0.995. The drug loading content (DLC), and the drug loading efficiency (DLE) were calculated from the following equations:

$$\text{Drug loading content}\ (\%) = \frac{\text{Weight of loaded drug in micelles(g)}}{\text{Weight of drug loaded micelles(g)}} \times 100$$

$$\text{Efficiency}\ (\%) = \frac{\text{Weight of loaded drug in micelles(g)}}{\text{Weight of drug added(g)}} \times 100$$

2.8. In vitro drug release

A dialysis bag (MWCO = 1000 Da) containing 6 mL of the drug loaded micelle suspension was sealed and immersed in a phosphate buffer solution (250 mL, 0.01 M, pH 7.4) at 37 °C in a thermostatically controlled bath. The copolymer concentration was 1% wt for PDMAEMA$_{co}$Cl(30) and (20) and 3.3% wt for PDMAEMA$_{co}$Cl(25). The ratio drug: copolymer was 1:5 (wt/wt) in all the experiments. After 24 h of dialysis, the dialysis cell was maintained into a freshly prepared 0.01 M PBS solution. Aliquots of 5 mL were withdrawn from the solution periodically. The volume of the solution was held constant by adding 5 mL fresh PBS solution after each sampling to ensure sink conditions. The amount of chlorambucil released from micelles was determined by fluorescence at 305 nm as excitation wavelength.

2.9. Measurements

^{1}H NMR and ^{13}C NMR spectra were recorded in D_2O solution on a Bruker AM-400 instrument at 400 MHz. IR spectra were recorded on a Perkin-Elmer FTIR-spectrophotometer and polymeric samples were examined as KBr discs. Elemental analysis: nitrogen and sulphur contents were determined by elemental analysis in a Micro-Carlo Erba equipment, model EA 1108. GPC molecular weights and polydispersity measurements were carried out using a Polymer Laboratories GPC system equipped with a differential refractive index and UV–vis detectors. Calibration was carried out using linear poly(methyl methacrylate) (PMMA) standards (Polymer Laboratories), ranging from 200 to 1.577×10^5 g mol^{-1}. The mobile phase was THF/triethylamine (5% v/v) at a flow rate of 1 mL min^{-1}. Triethylamine was added to circumvent adsorption of polyamine on the SEC columns. The system was equipped with a guard column PL-gel 5 μm and two C PL-gel 5 μm mixed columns in series, thermostated at 25 °C.

3. Results and discussion

3.1. Synthesis of the copolymers

ABA block copolymers were synthesized from difunctional macroinitiator PCL using copper-mediated living radical polymerization (LRP). Polymerization of (2-(*N,N*-dimethylamino)ethyl methacrylate was carried out at 80 °C in toluene using *N*-propyl-2-pyridinylmethyleneamine as a ligand [22] and Cu(I)Br. Table 1 summarizes feed composition (f_{DMAEMA}: molar fraction of DMAEMA in the feed), together with M_n and composition of copolymers (F_{DMAEMA}: molar fraction of DMAEMA in the copolymer) determined by GPC and by elemental analysis, respectively. The data confirm the absence of diblock copolymers. The copolymers were named as PDMAEMA$_{co}$(x), where x denoted the polymerization degree of each DMAEMA block.

Each polymerization was sampled with time and analyzed by ^{1}H NMR and GPC for measurement of conversion, molecular weight and polydispersity. Calculations were performed by ^{1}H NMR with comparison of the relative integration of the signals at 5.0 and 5.6 ppm assigned to the protons of monomeric double bond and that at 3.5 ppm for methylene protons of PDMAEMA. The kinetic plots, ln [M]/[M$_0$] versus time, for the polymerization of DMAEMA using different composition feeds are shown in Fig. 2 with linear plots indicating good first order kinetics and the concentration of growing radicals was constant during the reaction. All the polymers showed a relatively narrow molecular weight distribution and polydispersity ~1.2. These results suggest a controlled/living radical mechanism under these conditions.

Selective quaternization of PDMAEMA blocks was carried out by reaction with HCl to give rise to water-soluble PDMAEMA$_{co}$Cl copolymers. Also water-soluble PDMAEMA$_{co}$Q copolymers were obtained by reaction with methyl iodide. The polyelectrolytes were characterized by FTIR and ^{1}H NMR. In the FTIR spectrum, absorption at 2700 cm^{-1} from the ammonium group confirmed the structure of polyelectrolytes.

3.2. Polymeric micelles

The structures of the triblock copolymers were characterized by ^{1}H NMR. Assignments of methylene protons (1.2–1.6 and 2.2 ppm) for the PCL block and methyl protons (2.3 ppm) and methylene protons (2.5 ppm) for the PDMAEMA blocks are shown in Fig. 3, which showed successful formation of the triblock copolymer. In $CDCl_3$, where micellar formation was not expected, all ^{1}H NMR resonances attributed to PDMAEMA and PCL units were detected as shown in Fig. 3a. However, the ^{1}H NMR spectrum in D_2O showed an intensity reduction of PCL resonances due to suppressed molecular motion of the aggregated hydrophobic chains (Fig. 3b). ^{1}H NMR study in aqueous solution showed mainly hydrophilic PDMAEMA signals, strongly indicative of a core–shell type formation with a hydrophobic inner-core and a hydrophilic shell.

The formation of micelles from the triblock copolymers was also verified by and DLS measurements and fluorescence, using 4-(*N,N*′-diethyl)amino-7-nitrobenz-2-oxa-1,3-diazole (NBD-NEt$_2$) as fluorescent probe. At low concentrations, copolymer exists as unimers; self-assembly begins when the copolymer concentration reached the called cmc. The cmc of chlorohydrated and quaternized copolymers were determined by the fluorescence method described previously [23]. Fig. 4 shows the plots of the ratio of fluorescence quantum yields in presence and absence of copolymer versus copolymer concentration. From this plot was possible to determine the onset of microdomain formation put in evidence by the drastic slope change corresponding to the value of cmc (Table 2). At ambient temperature, the range of cmc's for

Table 1
Polymerization of DMAEMA using a difunctional macroinitiator based on PCL at 80 °C in toluene

Copolymers	f_{DMAEMA}[a]	F_{DMAEMA}[b]	$M_{n,th}$[c] (g/mol)	$M_{n,GPC}$[d] (g/mol)	PD	PI[d]	Conversion (%)
$PDMAEMA_{Co}(30)$	0.90	0.96	11100	11700	30	1.22	80
$PDMAEMA_{Co}(25)$	0.80	0.77	9800	10500	25	1.22	80
$PDMAEMA_{Co}(20)$	0.70	0.74	8780	9800	20	1.20	82

Polymerization degree (PD) of each DMAEMA block, molecular weight and molecular weight distribution of the triblock copolymers.
[a] Molar fraction of DMAEMA in the feed.
[b] Molar fraction of DMAEMA in the copolymer.
[c] $\overline{M}_{n,th} = (([Monomer]_0 \times M_{w,monomer} \times Conversion)/[Macroinitiator]_0) + \overline{M}_{n,macroinitiator}$.
[d] Determined by GPC, standards PMMA.

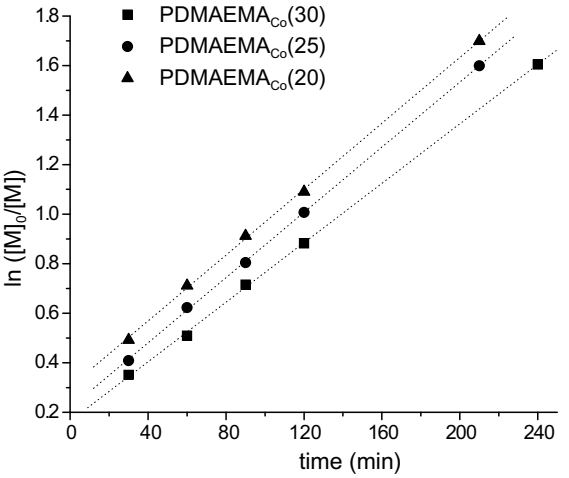

Fig. 2. Plot of ln $[M_0]/[M]$ against time for the polymerization of DMAEMA using different composition feeds.

copolymers = 0.11–1.01 g/L and highly dependent on the hydrophilic/hydrophobic balance in the copolymer molecule. As the length of the hydrophilic block PDMAEMA increases the cmc decreases.

In general, the cmc for $PDMAEMA_{co}Cl$ are lower than those for $PDMAEMA_{co}Q$ and the opposite trend is observed for the ratio of Φ_F/Φ_{F0}. This behaviour may be related to a looser polymeric micelles with a higher aggregation number for $PDMAEMA_{co}Q$ as a result of the higher size of the iodide anion compared with the chloride ion in $PDMAEMA_{co}Cl$. However, the values of cmc of $PDMAEMA_{co}Cl(20)$ and $PDMAEMA_{co}Q(20)$ were very close. Both copolymers exhibited a drastic increase of the fluorescence quantum yield at concentrations higher than the cmc, independently of the counter-ion of the ammonium group of PDMAEMA blocks. This pattern suggested that the repulsive interactions between hydrophilic segments are not affected by the counter-ion due to the shortest length of these blocks.

We also evaluated the mobility/rigidity of the polymeric micelles by using the fluorescent probe, NBD-NEt_2, which has been proven to be sensitive to mobility/rigidity changes in its microenvironment [24]. Fluorescence intensity increases due to the increasing viscosity surrounding the probe. This behaviour has been interpreted by assuming that the intramolecular charge transfer (ICT) excited

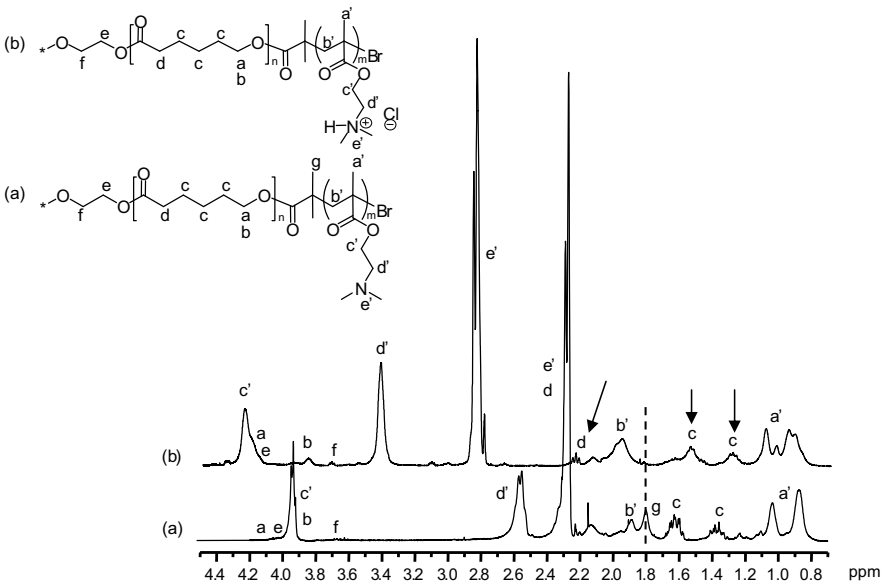

Fig. 3. ^1H NMR of the triblock copolymer $PDMAEMA_{Co}(25)$ in (a) $CDCl_3$ and (b) D_2O.

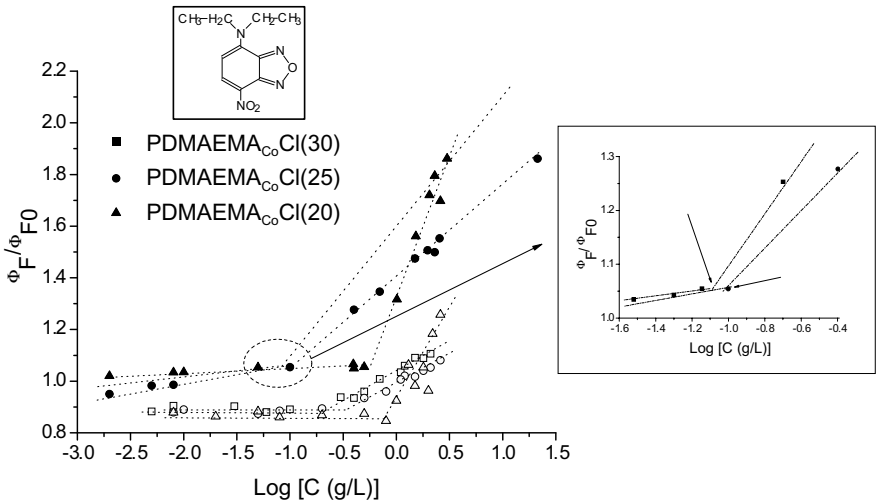

Fig. 4. Plots of the ratio φ_F/φ_{F0} against copolymer concentration for PDMAEMA$_{Co}$Cl copolymers (solid symbols) and PDMAEMA$_{Co}$Q copolymers (open symbols). The structure of the fluorescent probe NBD-NEt$_2$ is showed as an inset in the figure.

Table 2
Critical micellar concentrations (cmc in g/L) of PDMAEMA$_{co}$Cl and PDMAEMA$_{co}$Q triblock copolymers in the absence and presence of bovine serum albumin (BSA)

Copolymer	PDMAEMA$_{co}$Cl	PDMAEMA$_{co}$Cl in presence of BSA[a]	PDMAEMA$_{co}$Q
PDMAEMA$_{Co}$(30)	0.11	0.03	0.31
PDMAEMA$_{Co}$(25)	0.33	0.05	0.71
PDMAEMA$_{Co}$(20)	1.01	0.20	1.10

[a] [BSA] = 0.2 g/L.

state relaxes to a lower energy twisted intramolecular charge transfer (TICT) state by rotation about the amino group carbon–nitrogen bond. The radiative deactivation constant is not affected, but a decrease in the non-radiative deactivation constant is related to an increase in the viscosity [21]. Therefore, when the inner-core rigidity increases the slope of the plot of the ratio of fluorescence quantum yields versus copolymer concentration increases. At concentrations much greater than the cmc, the steepest slope was shown by the formation of PDMAEMA$_{co}$(20) micelles, indicating a tightly hydrophobic PCL core whereas the lowest slope corresponded to the formation of PDMAEMA$_{co}$(25) loose micelles.

It can not be excluded changes in the partition coefficient of the fluorescent probe depending on the copolymer. However, we were not succeeded to determine partition coefficient with this fluorescent probe in these systems. This fact was due to a continuous increase of fluorescence as the concentration of copolymer is increased up to 100 mg/mL and fluorescence intensity does not level-off. Therefore, the saturation intensity (the intensity for the probe does not change with increasing polymer concentration) was not reached for the range of copolymer concentration used in this work.

PDMAEMA$_{co}$Cl block copolymers and proteins share a common property of both charged groups and hydrophobic regions. This implies that the solution properties might be very different than those of individual solutions. The micellization onset of PDMAEMA$_{co}$Cl in presence of a protein, bovine serum albumin (BSA), was studied and data are compiled in Table 2. The plot of the ratio of Φ_F/Φ_{F0} versus copolymer concentration defined a clear breakpoint when a certain copolymer concentration was reached. The beginning of the interaction between copolymer and protein was typically displayed as critical aggregation concentration (cac) which lay below the cmc of the respective copolymers. At neutral pH BSA is negatively charged and copolymers are cationic. Therefore, cooperative binding of molecules can be induced hydrophobically and/or electrostatically. It is suggested that the surfactant molecules in our present studies bind to form the micelle-like clusters in the protein–surfactant complex.

The micelles formed of PDMAEMA$_{co}$Cl copolymers were studied by dynamic light scattering in order to measure their effective diameter and their population distribution in terms of size. Fig. 5 shows the population distribution of the micelles calculated by CONTIN analysis of the dynamic light scattering measurements. The micelles exhibited a distinct size distribution pattern depending on their composition. In PDMAEMA$_{Co}$Cl(25) copolymer, a bimodal size distribution was observed, most of the population had a mean diameter of about 150 nm, and the remaining population exhibited smaller size of about 30 nm. Bimodal distributions have been obtained for other polymer micelles such as amphiphilic di and triblock copolymers of styrene and quaternized 5-(*N*,*N*-diethylamino) isoprene in selective solvents [25]. The largest size aggregates were observed for PDMAEMA$_{Co}$Cl(30) copolymer with more complex size distribution. An opposite trend was observed for PDMAEMA$_{Co}$Cl(20) showing a narrow and monodispersed size distribution.

Generally, the size of core–shell type polymeric micelles lies in the range of several tens of nanometers. Therefore, the larger size fraction of population corresponds to supramolecular structures formed by an intermolecular

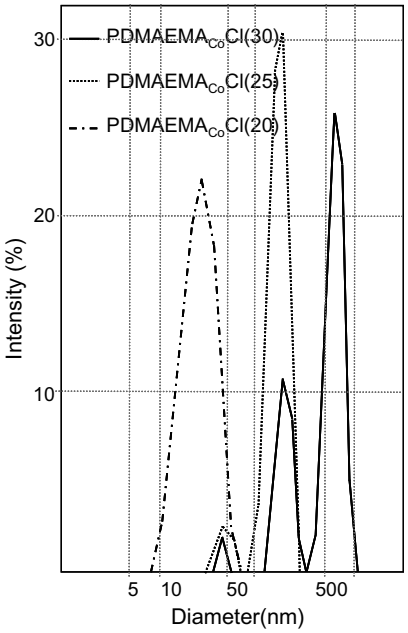

Fig. 5. Population distribution of the micelles calculated by CONTIN analysis of the dynamic light scattering measurements.

aggregation process. Particles exceeding 100 nm are aggregates that result from intermicelle association and hydrophobic interactions between the exposed cores of micelles [26]. We believe that secondary aggregation might be strongly favoured when PDMAEMA is used as the peripheral block because of its amphiphilic nature. The extension of the ionic block played a key role in tuning the size of micelles. As polymerization degree of PDMAEMA block increased the systems attempted to decrease the total interfacial area, and micelles fusion occurred, resulting in an increase in the micelles size and a decrease of the total number of particles. The aggregates showed a spherical morphology (Fig. 6a) and a close inspection of the TEM micrograph showed secondary aggregation as well (Fig. 6b). Hence, the maximum value of the theoretical micellar diameter (D_h th) was calculated as the sum of the length of the PCL central block and twice the length of the peripheral block. The length of each block was determined by the product of polymerization degree multiplied by the polydispersity degree and by the contribution of a monomeric repetition unit to the chain length (0.2546 nm). For all the copolymers, the value of the mean diameter corresponding to the smallest aggregates is closed to that estimated from a spherical model micelle (Table 3).

3.3. Thermoresponsive behaviour

To determine whether these micelles exhibit a thermal sensitivity as expected [27], we further examined the optical transmittance of a polymeric micelle PBS solution (pH 7.4) as a function of temperature. Concentration of polymeric solutions (1.5 g/L) was chosen well-above cmc of all the copolymers to ascertain the formation of polymeric micelles. Whilst the PCL block is hydrophobic, the PDMAEMA blocks are hydrophilic at ambient temperature and

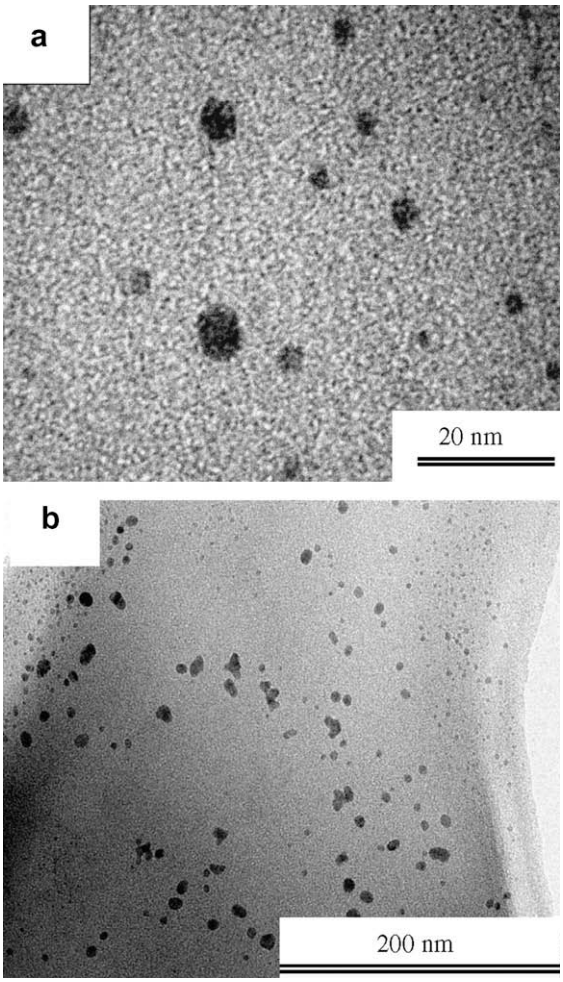

Fig. 6. TEM images of the resulting micelles self-assembled of PDMAEMA$_{Co}$Cl(25) in aqueous media.

become hydrophobic above the demixing temperature as a result of the lower critical solution temperature (LCST) behaviour. The *%T* changes as a function of temperature of PDMAEMA$_{co}$Cl aqueous solutions measured at 550 nm, Fig. 7. PDMAEMA$_{co}$Cl block copolymers are thermal-sensitive polymers exhibiting LCST. These micelles underwent a change in their structure at different temperatures, between 54 and 87 °C, depending on their composition. And PDMAEMA$_{Co}$Cl(25) exhibited the lowest LCST (54 °C) in accordance with the lowest rigidity of these micelles.

Moreover, the soluble–insoluble change was entirely reversible without hysteresis for PDMAEMA$_{Co}$Cl(30) as

Table 3
Hydrodynamic diameter of copolymer micelles determined by dynamic light scattering (D_h) and theoretical hydrodynamic diameter calculated assuming a spherical morphology of micelles

Copolymer	D_h (nm)	D_h th (nm)
PDMAEMA$_{Co}$Cl(30)	30 ± 6	24
PDMAEMA$_{Co}$Cl(25)	28 ± 6	21
PDMAEMA$_{Co}$Cl(20)	17 ± 4	18

demonstrated by the transition from a turbid solution to a transparent solution when the aqueous temperature was decreased from above to below the LCST. However, the thermoresponsive behaviour was found reversible with a slower response rate as the length of hydrophilic block decreased for the other triblock copolymers. We suggest that the coronas of the micelles were crowded in a way that could hinder the relaxation of PDMAEMA blocks. Similar behaviour was observed for poly(styrene-b-*N*-isopropylacrylamide) [28]. The influence of macromolecular architecture on the thermal response rate of amphiphilic copolymers based on poly(*N*-isopropylacrylamide) and poly(oxyethylene) in water has been recently studied [29]. These authors found that the thermal response of graft copolymers is faster than that of block copolymers.

3.4. Drug loading efficiency

Dialysis is an effective method for drug loading into micelles and for assessing the in vitro drug release. Chlorambucil was solved in ethanol and added to the copolymer solution; followed by dialysis of this solution against phosphate buffer solution. A gradual replacement of the organic solvent with water triggered self-assembly of hydrophobic PCL blocks accompanied by the entrapment of drug in micelles cores. The drug loading efficiency, cmc and a factor *F* defined by the ratio between the initial copolymer concentration and its cmc are listed in Table 4.

The drug loading efficiency (DLE) varied between 30% and 78%. By increasing weight ratio of drug to polymer increased DLE. For example, in the case of PDMAEMA$_{Co}$Cl(25), the feed weight ratio of chlorambucil to polymer increased from 0.2 to 0.66, the DLE increased from 39% to 78%. Also, the drug loading efficiencies depended on composition of block copolymer. For PDMAEMA copolymers, PDMAEMA$_{Co}$Cl(25) has the highest DLE while PDMAEMA$_{Co}$Cl(30) shows the lowest DLE. It is well-known that the interactions between the drug and the core block determine the encapsulation of the drug [30]. Chlorambucil is inherently hydrophobic due to its chemical structure and possess a carboxylic acid group. The presence of water inside the hydrophobic core may be very low, avoiding the hydration of carboxylic acid groups of drug and resulting in the hydrogen bond formation between the carbonyl moieties of PCL and the acid group of chlorambucil, Fig. 8. The specific interaction is expected to work preferentially for drug incorporation without producing precipitates which can be frequently seen in cases of non-specific hydrophobic interactions. Therefore, physical entrapment of hydrophobic drugs into micelles is believed to be driven by hydrophobic interactions and hydrogen bonds between drug and hydrophobic core. Moreover, this interaction between drug-polymeric micelles may influence on the drug release behaviour.

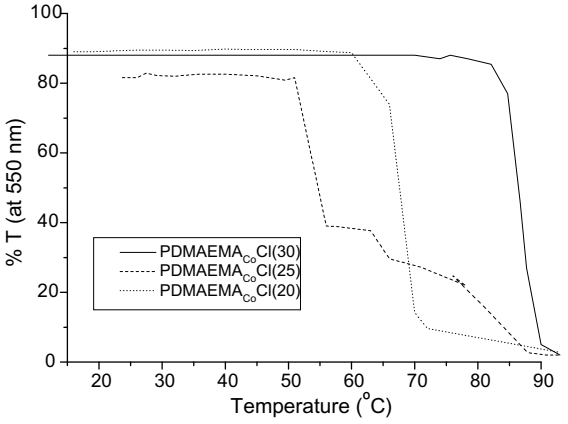

Fig. 7. Thermoresponsive behaviour of self-assembled micelles upon temperature changes.

The nature of the shell was found to play a key role in self-assembly behaviour and DLE decreased considerably for PDMAEMA$_{Co}$Q(25) compared to the counterpart PDMAEMA$_{Co}$Cl(25) (Table 3). Taking into account that the length of the hydrophobic block based on PCL was maintained constant in all the copolymers, the expansion of micelle shell may cause hindrance to drug encapsulation resulting in lower DLE.

3.5. In vitro chlorambucil release studies

The time-dependent drug release profile of the micelles in 0.01 M PBS aqueous solution at 37 ± 1 °C was studied, Fig. 9. Interestingly, the PDMAEMA$_{Co}$Cl(20) micelles released chlorambucil in a sustained manner over more than 100 h. In contrast, a relatively rapid release was observed within the first 24 h, followed by slow, sustained release over a 4-day period, from PDMAEMA$_{Co}$Cl(30) micelles. The release rates were very different, even if the initial drug loading was the same. In fact, during the first 24 h of exposure, the PDMAEMA$_{Co}$Cl(30) micelles showed a 70% of released drug, compared with a 22% released from the PDMAEMA$_{Co}$Cl(20) micelles Surprisingly, the release behaviour from PDMAEMA$_{Co}$Cl(25) followed an accelerated process after a short induction period. This pattern is explained by the formation of aggregates with different sizes, as confirmed by DLS. In comparison to the release behaviour from a monodispersed sample, the presence of a particle size distribution causes a substantial acceleration of the transport at early times [31].

In order to investigate the mechanism of drug release and to compare the performance of various copolymers micelles, the percentage of drug released versus time profiles were used. Data corresponding to 5–60% release showed a good fit to the Power Law Model [32] expressed in the following equation:

$$\frac{M_t}{M_\infty} = k \cdot t^n$$

Table 4
Drug loading content and efficiency (DLC and DLE), cmc and a factor *F* (*F* = [copolymer]$_0$/CMC) of the PDMAEMA$_{Co}$ micelles

Copolymer	cmc (g/L)	Factor	DLC (%)	DLE (%)
PDMAEMA$_{Co}$Cl(30)	0.11	100	4.8	29
PDMAEMA$_{Co}$Cl(25)	0.33	30	6.6	39
		100	13.0	78
PDMAEMA$_{Co}$Cl(20)	1.01	10	5.6	34
PDMAEMA$_{Co}$Q(25)	0.71	14	0.5	3

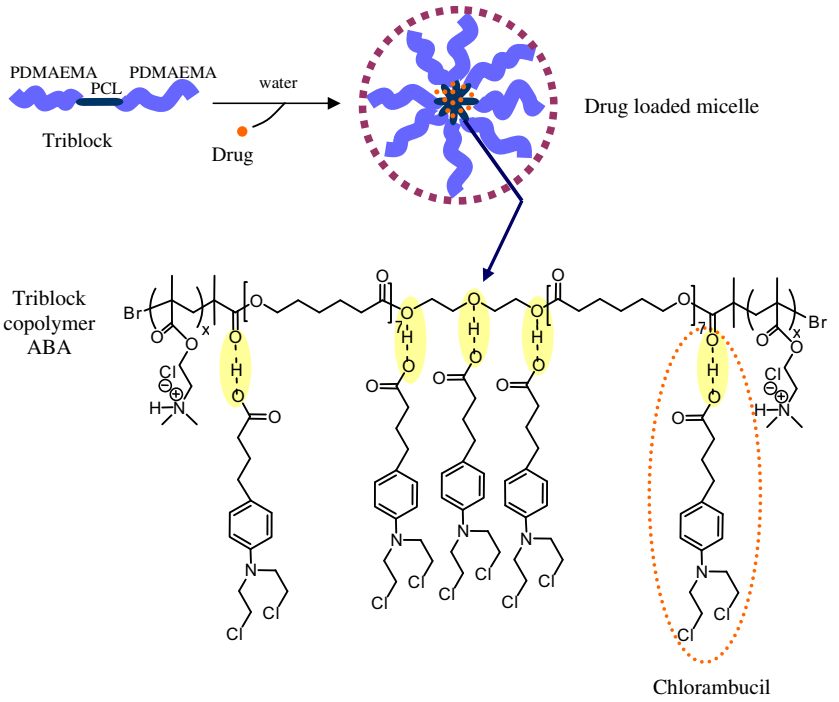

Fig. 8. Specific interaction between drug and micelles due to the hydrogen bond formation between the carbonyl moieties of PCL and the acid group of chlorambucil.

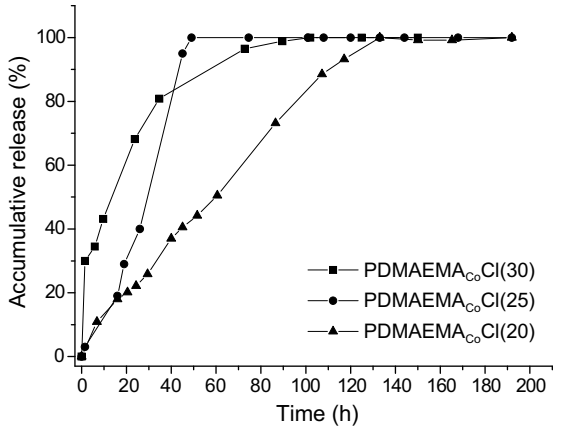

Fig. 9. Drug release profiles from micelles formed by triblock copolymers PDMAEMA$_{Co}$Cl containing chlorambucil.

where M_t was the amount of drug released at time t, M_∞ was the amount of drug released after infinite time, k was a kinetic constant incorporating structural and geometric characteristics of the system, and n was the diffusional exponent indicative of the drug release mechanism. For spherical geometry, values of n value between 0.43 and 0.85 can be regarded as an indicator for the superposition of two phenomena (diffusion-controlled and swelling-controlled drug release) [31]. The values of the kinetic constant (k), the release exponent (n) and correlation coefficient (R^2) were determined according to this equation from the drug release profiles. The correlation coefficients for the data were >0.99 and illustrated that the release were predictive by the empirical exponential equation. Values of n equals to 0.73 for PDMAEMA$_{Co}$Cl(20) and 0.5 for PDMAEMA$_{Co}$Cl(30) indicated anomalous transport and the release was controlled by a combined degradation–diffusion mechanism in all cases. The degradation or erosion can be caused by deagglomeration and/or chemical hydrolysis of PCL core. Taking into account the suspensions showed secondary aggregation (TEM images), the surface area of the system is also responsible for the different burst release and the mechanism could be related to both particle deagglomeration and drug diffusion.

Homopolymer PCL is a highly hydrophobic material with a slow in vitro hydrolytic degradation rate. After attaching hydrophilic DMAEMA blocks at both extremes of the linear PCL, the resultant copolymers became more hydrophilic compared with PCL. The hydrolytic stability of the polymeric micelles was dependent on the length of the hydrophilic blocks. This behaviour and biodegradability is currently under investigation. We have observed that different genera of bacteria, such as *Pseudomonas* and *Bacillus*, grew in aqueous solutions in the presence of these amphiphilic copolymers. Surprisingly they are biodegraded below cmc and also, above cmc.

4. Conclusions

A series of novel amphiphilic triblock copolymers based on 2-(*N*,*N*-dimethylamino)ethyl methacrylate and ε-caprolactone were designed and synthesized. Thermosensitive triblock copolymers self-assembled into supramolecular aggregates in aqueous solution and exhibited cmc's rang-

ing from 0.11 to 1.01 g/L. In presence of proteins, PDMAEMA block copolymers formed micelle-like clusters by cooperative binding. Investigation of polymeric micelles in aqueous medium showed that the composition of the hydrophilic segment has a significant influence on its physicochemical characteristics. These polymeric micelles were loaded with an anticancer drug, chlorambucil. The drug loading efficiency of PDMAEMA micelles was optimized by entrapping the poorly water-soluble drug containing functional groups capable to interact by hydrogen bonds with the PCL core-forming block. Comparing to other PCL copolymers, the PDMAEMA copolymers exhibited smaller cmc's and better drug loading properties. The role of secondary aggregation in the drug incorporation was put in evidence.

The control of the drug release kinetics can be achieved by optimizing the composition of the used polymers and the particle size of the nanoparticles. For example, PDMAEMA$_{Co}$Cl(20) micelles could prove useful for drug delivery applications as a very sustained release from a very small drug reservoir is required for its drug targeting, which indicated that the nanoparticles were very suitable for delivery carriers of hydrophobic probes.

Acknowledgements

The authors thank the Plan Nacional I + D + I (Ministerio de Educación y Ciencia) for financial support (MAT2006-05979) as well as the Comunidad Autónoma de Madrid for the funding through I + D Program (S0505/MAT-0227).

References

[1] Alexandridis P, Lindman B, editors. Amphiphilic block copolymers: self-assembly and applications. Amsterdam: Elsevier Science; 2000.
[2] Hillmyer MA. Science 2007;317:604–5.
[3] Rapport N. Prog Polym Sci 2007;32:962–90.
[4] Chen C, Yu CH, Cheng YC, Yu PHF, Cheung MK. Biomaterials 2006;27:4804–14.
[5] Kakizawa Y, Kataoka K. Adv Drug Deliv Rev 2002;54:203–22.
[6] Kumar N, Ravikumar MNV, Domb AJ. Adv Drug Deliv Rev 2001;53:23–44.
[7] Béduneau A, Saulnier P, Benoit JP. Biomaterials 2007;28:4947–67.
[8] Vakil R, Kwon GS. J Control Release 2005;101:386–9.
[9] Yu H, Gan LH, Hu X, Venkatraman SS, Tam KC, Gan YY. Macromolecules 2005;38:9889–93.
[10] Zheng G, Stover HDH. Macromolecules 2003;36:7439–45.
[11] Du J, Tang Y, Lewis AL, Armes SP. J Am Chem Soc 2005;127:17982–3.
[12] Weaver JVM, Armes SP, Bütün V. Chem Commun 2002;18:2122–3.
[13] Lowe AB, Billingham NC, Armes SP. Macromolecules 1998;31:5991–8.
[14] Liu S, Weaver JVM, Tang Y, Billingham NC, Armes SP, Tribe K. Macromolecules 2002;35:6121–31.
[15] Yuan W, Yuan J, Zheng S, Hong X. Polymer 2007;48:2585–94.
[16] Zhang F, Wu Q, Chen Z, Zhang M, Lin X. J Colloid Interface Sci 2008;317:477–84.
[17] Sinha VR, Bansal K, Kaushik R, Kunria R, Trehan A. Int J Pharm 2004;278:1–23.
[18] Keller RN, Wycoff HD. Inorg Synth 1947;2:1.
[19] Haddleton DM, Crossman MC, Dana BH, Duncalf DJ, Heming AM, Kukulj D, et al. Macromolecules 1999;32:2110–9.
[20] Motala-Timol S, Jhurry D. Eur Polym J 2007;43:3042–9.
[21] Fery-Forgues S, Fayet JP, Lopez A. J Photochem Photobiol A Chem 1993;70:229.
[22] Limer A, Haddleton DM. Prog React Kinet Mec 2004;29:187–241.
[23] Alonso A, Catalina F, Salvador EF, Peinado C. Macromol Chem Phys 2001;202:2293–9.
[24] Peinado C, Alonso A, Salvador EF, Baselga J, Catalina F. Polymer 2002;43:5355–61.
[25] Riegel IC, Samios D, Petzhold CL, Eisenberg A. Polymer 2003;44:2117–28.
[26] Allen C, Yu Y, Maysinger D, Eisenberg A. Bioconj Chem 1998;9:564–72.
[27] Liu S, Billingham NC, Armes SP. Angew Chem Int Ed 2001;40:2328.
[28] Nuopponen M, Ojala J, Tenhu H. Polymer 2004;45:3643–50.
[29] Van Durme K, Van Assche G, Aseyev V, Raula J, Tenhu H, Van Mele B. Macromolecules 2007;40:3765–72.
[30] Giacomelli C, Schmidt V, Borsali R. Langmuir 2007;23:6947–55.
[31] Ritger PL, Peppas NA. J Control Release 1987;5:23–36.
[32] Spiepmann J, Peppas NA. Adv Drug Deliv Rev 2001;48:139–57.